Structural Characterization of Two Interchangeable Conformations of a 2-Aminofluorene-Modified DNA Oligomer by NMR and Energy Minimization†

Linda M. Eckel and Thomas R. Krugh*

Department of Chemistry, University of Rochester, Rochester, New York 14627

Received May 23, 1994; Revised Manuscript Received August 25, 1994®

ABSTRACT: One- and two-dimensional NMR spectroscopy and energy minimization calculations were used to investigate the conformation of a 2-aminofluorene- (AF-) modified model human c-H-*ras*1 protooncogene codon 61 deoxyoligonucleotide duplex, d(C1-A2-C3-C4-A5-{AF-G6}-G7-A8-A9-C10)·d(G11-T12-T13-C14-C15-T16-G17-G18-T19-G20), in which the AF adduct is located at the third base of codon 61 with cytosine as the complementary nucleotide. Two interchangeable conformations of the AF-modified duplex, referred to as the external-AF conformation and the inserted-AF conformation, were determined from the NMR data. An analysis of the coalescence of resonances led to the estimation that the chemical exchange lifetime is greater than 3 ms but less than 20 ms at 30 °C, pH 7. In the external-AF conformation, Watson−Crick base-pair formation is observed for all 10 complementary nucleotides, including the AF-G6·C15 base pair. In the inserted-AF conformation, 9 of the 10 complementary bases form Watson−Crick base pairs; the AF-G6 imino proton exhibits no evidence of hydrogen bond formation with its complementary cytosine. Several NOEs between aminofluorene protons and DNA protons show that the AF moiety in the inserted-AF conformation stacks between the adjacent A5·T16 and G7·C14 base pairs. Solvated energy minimization calculations using distance restraints obtained from NOESY data at 2 °C with a 100-ms mixing time were performed to obtain representative structures of the external-AF and inserted-AF conformations. The external-AF conformer has the AF moiety protruding out of the major groove of a relatively unperturbed DNA duplex, leaving intact Watson−Crick base pairing for the AF-G6·C15 bases. Thus, the external-AF conformer may represent a visualization of a conformation that allows faithful replication. The inserted-AF conformer has the AF moiety stacked within the DNA helix, breaking the Watson−Crick base pairing of the modified guanine and its complementary cytosine and displacing the guanine and cytosine into the grooves. We label the inserted-AF conformer as a premutagenic conformation to reflect the displacement of the modified guanine. Interconversion between the structurally distinct external-AF and inserted-AF conformers takes place on a time scale of the same order as DNA replication. We have labeled this interconversion as a mutagenic switch to highlight a possible conformational equilibrium that may be important in replication.

Chemical carcinogens that covalently bind to DNA may result in base substitutions, frame-shift mutations, deletions, or gene rearrangements within the cell (Beland & Poirier, 1989; Selkirk, 1980; Weinstein, 1981). 2-Aminofluorene (AF),[1] an aromatic amine, and the related *N*-acetyl-2-aminofluorene (AAF) have been extensively studied as model chemical carcinogens since the discovery of their ability to induce a variety of tumors in laboratory animals during toxicity testing as a potential insecticide in the 1940s (Kriek, 1992; Miller, 1970; Weisburger & Weisburger, 1958; Wilson et al., 1941). AF and AAF are metabolically activated *in vivo* to a reactive intermediate which then covalently binds to DNA, primarily at the C8 position of guanine (Beland & Kadlubar, 1990; Miller & Miller, 1967; Singer & Grunberger, 1983). *N*-(Deoxyguanosin-8-yl)-2-aminofluorene DNA adducts (Figure 1) are persistent in mammalian systems (Gupta & Dighe, 1984; Poirier et al., 1982) and have been shown to induce base substitution or frame-shift mutations during DNA replication (Bichara & Fuchs, 1985; Carothers et al., 1993; Mah et al., 1989; Reid et al., 1990), although translesion bypass with correct incorporation of cytosine opposite the modification site is the predominant outcome (Lutgerink et al., 1985; Michaels et al., 1991; Shibutani & Grollman, 1993; van de Poll et al., 1992).

Investigations of AF-G adducts using experimental and theoretical techniques have resulted in a variety of proposed conformers. Early experimental work (Fuchs & Daune, 1974; Kriek & Spelt, 1979; Leng et al., 1980; Sage et al., 1979; Santella et al., 1980) indicated that AF modification of DNA caused less distortion of the duplex with less stacking of the fluorene moiety than the bulkier acetylated adduct in which AAF-G rotates to a *syn* domain and the fluorene moiety stacks within the duplex (Fuchs & Daune, 1972; Grunberger et al., 1970). One-dimensional NMR and CD experiments (Evans et al., 1980; Leng et al., 1980) of

† This publication was supported by Grant CA35251 from the National Cancer Institute. Its contents are solely the responsibility of the authors and do not necessarily represent the official views of the National Cancer Institute.

® Abstract published in *Advance ACS Abstracts,* October 15, 1994.

[1] Abbreviations: AF, 2-aminofluorene; AAF, *N*-acetyl-2-aminofluorene; AAAF, *N*-acetoxy-2-(acetylamino)fluorene; AF-G, AF-modified guanine DNA oligomer; AAF-G, AAF-modified guanine DNA oligomer; CD, circular dichroism; dG-AF, *N*-(deoxyguanosin-8-yl)-2-aminofluorene; dG-AAF, *N*-(deoxyguanosin-8-yl)-2-(acetylamino)-fluorene; NMR, nuclear magnetic resonance; TSP, sodium 3-(trimethylsilyl)propionate-*2,2,3,3-d*$_4$; NOE, nuclear Overhauser effect; NOESY, nuclear Overhauser effect spectroscopy; ROESY, rotating-frame Overhauser effect spectroscopy; TOCSY, total correlation spectroscopy; DQFCOSY, double-quantum-filtered correlation spectroscopy.

0006-2960/94/0433-13611$04.50/0

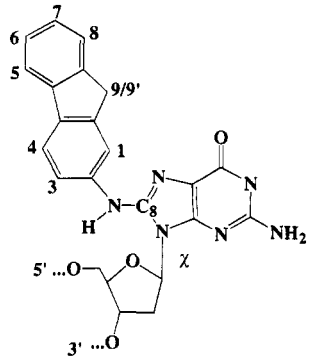

FIGURE 1: Chemical structure of the *N*-(deoxyguanosin-8-yl)-2-aminofluorene DNA adduct. The glycosidic torsion angle of the AF-G residue is labeled as χ.

AF-modified guanosine indicated the glycosidic torsion angle was preferentially in the *anti* domain. Evans (1980) reported that the *anti* conformation created little steric interference in a space-filling model in which the modified guanine remains Watson–Crick base paired while the AF moiety is in the major groove of a B-form DNA duplex. Extensive theoretical analyses of AF-modified duplexes found several low-energy conformations in which the AF-modified guanine was in either an *anti* or *syn* glycosidic torsion domain with the fluorene moiety or the modified guanine in a stacked position (Broyde & Hingerty, 1983, 1984; Hingerty & Broyde, 1982, 1986; Lipkowitz et al., 1982). Spectroscopic techniques were used to study the conformational changes induced by AF modification of DNA and poly[d(G-C)]·poly-[d(G-C)], and it was concluded that the AF moiety was inserted within the B-form helix with the AF-G glycosidic angle in the *syn* domain (van Houte et al., 1987, 1988). More recently, van Houte et al. (1991) studied an AF-modified trinucleotide and found an *anti* AF-G conformation. Patel and co-workers (Norman et al., 1989) employed NMR spectroscopy and energy minimization calculations on an 11-mer duplex containing adenine opposite an AF-modified guanine to determine a structure in which the modified guanine is in a *syn* conformation with the aminofluorene ring located within the minor groove of the duplex without overlapping the aromatic rings of the adjacent base pairs. Thus, previous studies reveal a diversity of possible AF-G conformations—the AF moiety may be inserted within the helix or unstacked in either the major or minor groove, with the glycosidic torsion angle of the AF-modified guanine in either the *anti* or *syn* domain.

Interconversion between different AF-G conformers of AF-modified duplexes has been proposed (Broyde & Hingerty, 1983, 1984; Lipkowitz et al., 1982). Broyde and Hingerty (1983) found two types of low-energy *anti*-domain AF-G conformations in which the fluorene moiety could readily move from an unstacked position in the major groove to a stacked position above the adjacent base without necessarily causing disruption of the AF-G·C base pair and discussed the possible impact of the equilibrium on mutagenesis. Conformational mobility of AF-modified and AAF-modified oligomer duplexes has been observed in two-dimensional NMR (Norman et al., 1989; O'Handley et al., 1993) and CD studies (van Houte et al., 1989, 1991). In a preliminary report (Eckel & Krugh, 1994), we described the interconversion observed between two conformations of the AF-modified duplex that is discussed in detail within this paper. Cho and co-workers (1994) independently investigated an AF-modified 15-mer duplex with two-dimensional NMR spectroscopy and found evidence for at least two conformations; in one form the AF moiety is in the major groove of a relatively undisturbed B-type duplex, while the other form contains a stacked AF fragment.

Chart 1: Sequential Numbering of the AF-Modified 10-mer Duplex

AF

5′ C1 – A2 – C3 – C4 – A5 – G6 – G7 – A8 – A9 – C10 3′

3′ G20 – T19 – G18 – G17 – T16 – C15 – C14 – T13 – T12 – G11 5′

Mutational studies involving the modification of mammalian c-H-*ras*1 protooncogenes with an activated form of the aromatic amine demonstrated that the majority of mutations induced occur at codon 61 (Vousden et al., 1986; Wiseman et al., 1986). An oligonucleotide containing the sequence of codons 60–62, 5′GGC CAG GAG3′, was synthesized and reacted with *N*-acetoxy-2-(acetylamino)-fluorene (AAAF). Reaction of AAAF with this guanine-rich oligomer, however, resulted in a complex mixture of modified oligomers. To simplify HPLC purification of the reaction mixture, the terminal guanines were replaced with cytosine or adenine while the crucial sequence around the modification site (the third base of codon 61) was retained. The resulting oligonucleotide sequence, 5′CAC CAG GAA C3′ (underline indicates the DNA bases that are the same as the codon 60–62 sequence), was instead used to investigate an 2-aminofluorene–guanine adduct in a model human c-H-*ras*1 protooncogene codon 61 oligomer duplex.

The sequence and numbering scheme of the AF-10-mer used for the NMR experiments are shown in Chart 1. This AF-modified duplex has cytosine (C15) as the complementary nucleotide and is thus representative of an AF lesion site either prior to DNA replication or after faithful replication. NMR analysis of this AF-10-mer demonstrates the existence of two conformations, referred to as the external-AF conformation and the inserted-AF conformation. In the external-AF conformation, the modified guanine forms a Watson–Crick base pair with the AF moiety protruding out of the major groove of a B-form DNA oligomer duplex. In the inserted-AF conformation, the AF moiety is stacked with the adjacent bases, displacing the modified guanine and its complementary cytosine. Interconversion between the two conformations was established by the observation of chemical exchange cross-peaks in two-dimensional nuclear Overhauser effect (NOESY) and rotating-frame nuclear Overhauser effect (ROESY) experiments at 10, 20, and 30 °C. The chemical exchange lifetime is estimated to be in the range of 3–20 ms at 30 °C, thus creating the possibility of a conformationally significant structural change on a time scale similar to DNA synthesis (Kornberg & Baker, 1992). Interconversion between the two conformers of an AF-modified duplex provides a visualization for rationalizing error-prone and error-free replication of a duplex containing an AF-G adduct. We label this interconversion as a mutagenic switch because it takes place on a time scale similar to that of replication and thus may reflect a potential conformational equilibrium at a replicating fork.

MATERIALS AND METHODS

Materials. *N*-Acetoxy-2-acetylaminofluorene (AAAF) was purchased from the National Cancer Institute repository operated by Midwest Research Institute. The deoxyoligonucleotides d(CACCAGGAAC) and d(GTTCCTGGTG)

were synthesized by the phosphoramidite method (Caruthers et al., 1987) on a Pharmacia DNA synthesizer using Cruchem reagents.

Purification of Oligonucleotides. The oligomer was cleaved from the silica support and the amino protecting groups were removed by heating the sample at 55 °C for 18 h in concentrated aqueous ammonium hydroxide. The ammonium hydroxide was removed by evaporation and the sample filtered through a 0.45-μm Spin-X nylon membrane (Costar Co.) to remove any remaining silica. After the last coupling reaction, the 5′-terminal 4,4′-dimethoxytrityl (DMT) group was retained on the complete oligomer, and therefore, separation from the failure sequences using reverse-phase HPLC on a semipreparative PRP-1 (305 × 7 mm i.d., Hamilton Co.) polystyrene column could be achieved (Huang & Krugh, 1990). The mobile phase consisted of buffer A (0.01 M potassium phosphate, pH 7) and buffer B (70% acetonitrile, 10% methanol, and 20% buffer A). A solvent gradient of 5% B to 40% B in 30 min at 2 mL/min separated the nontritylated failure sequences from the desired trityl-bearing oligomer. The recovered sample was desalted using a disposable C18 Sep-Pak cartridge (Waters Co.) and the 5′-DMT group was cleaved with 80% acetic acid (60 min at room temperature). The acetic acid was removed by evaporation and the DMT group extracted with water-saturated diethyl ether. The purified oligomers were desalted with disposable Sep-Pak reverse-phase C18 cartridges.

Preparation of the N-Acetyl-2-aminofluorene Adduct. The purified d(CACCAGGAAC) oligomer was dissolved in 0.01 M potassium phosphate buffer (pH 7) to give a DNA concentration of approximately 1 mM. The oligomer solution was purged with argon. AAAF was dissolved in absolute ethanol (final reaction solution 15% ethanol) and then added to the oligomer solution to give a 4:1 ratio of AAAF to DNA. The reaction proceeded for 4 h at 37 °C. The unreacted AAAF was extracted with water-saturated diethyl ether. The remaining aqueous reaction mixture was purified by reverse-phase HPLC. Although the retention times of the monoguanine adducts d(CACCA{AAF-G}-GAAC) and d(CACCAG{AAF-G}AAC) are similar (21.6 and 22.6 min, using the gradient described above), separation of these two adducts was possible; the diguanine adduct d(CACCA{AAF-G}{AAF-G}AAC) has a longer retention time (32.7 min), facilitating its separation (Figure A, supplementary material). Using a 4:1 AAAF to DNA reaction ratio with the given conditions, approximately 50% of the DNA remains unreacted with a 20% yield of each monoguanine adduct and a 10% yield of the diguanine adduct. The purity of each isolated monoguanine *N*-acetyl-2-aminofluorene-modified adduct was verified by HPLC; then each sample was desalted using Sep-Pak C18 cartridges.

Preparation of the 2-Aminofluorene Adduct. Each purified AAF-modified oligomer was deacetylated in a 1 M NaOH solution containing 3% (v/v) 2-mercaptoethanol to minimize oxidative degradation during the deacetylation reaction (Shibutani et al., 1990). The reaction was allowed to proceed for 1 h, neutralized with dilute (10%) hydrochloric acid, and purged with argon for 3 h. Each 2-aminofluorene-modified oligomer was purified by reverse-phase HPLC, characterized with UV absorbance (Johnson et al., 1987; Shibutani et al., 1991; Spodheim-Maurizot et al., 1979), and desalted using disposable Sep-Pak C18 cartridges.

Duplex Formation. The 1:1 stoichiometric ratio for duplex formation was determined by titrating the AF-modified oligomer against its complementary sequence. The end point was monitored with one-dimensional NMR spectroscopy by observing the disappearance of the aggregated and non-hydrogen-bonded imino resonances and the appearance of the hydrogen-bonded imino resonances after each small addition of the modified oligomer to its complementary sequence.

NMR Experiments. All NMR experiments were performed on a 500-MHz Varian VXR-500S NMR spectrometer. Experiments were performed in either D_2O or 9:1 H_2O/D_2O (v/v) solution. The AF-modified duplex and the unmodified duplex samples were prepared in a 0.01 M sodium phosphate, 0.1 M sodium chloride, and 0.001 M EDTA buffer solution, pH 7. The sample concentration for the AF-modified duplex was 2.5 mM in 400 μL of the buffer solution. Chemical shift values are given relative to the sodium 3-(trimethylsilyl)propionate-*2,2,3,3-d*$_4$ (TSP) resonance referenced at 0.0 ppm.

One-Dimensional H_2O Experiments. One-dimensional proton spectra in H_2O solution were recorded with 22K data points over an 11 000-Hz sweep width at several temperatures (0−55 °C). The transmitter frequency was set on the H_2O resonance, and the offset was set at 4000 Hz to maximize the signal from the imino proton resonances (10−15 ppm). The H_2O resonance was suppressed with a 1331 pulse sequence (Hore, 1983). One-dimensional NOE experiments were recorded with the same NMR parameters and displayed as difference spectra. Individual resonance saturation (70%) was achieved by irradiation of the resonance with low power from the decoupler channel for suitable times (0.2−1.5 s).

NOESY 11 Echo Experiments. Two-dimensional phase-sensitive proton NOESY experiments were recorded in H_2O solution with 100- and 125-ms mixing times at 10 and 2 °C, respectively, with a 1-1 echo pulse sequence (Sklenar & Bax, 1987) incorporated for solvent suppression. The water resonance was partially saturated for 0.5 s during the relaxation delay. A sweep width of 12 000 Hz was used in both dimensions. A total of 4096 points were collected in the t_2 dimension, 512 t_1 values were collected for each data set, and 64 transients were collected for each t_1 value. The data were apodized with a Gaussian function (gf = 0.079) in the t_2 dimension and a shifted sine-bell function (sb1 = −0.019; sbs1 = −0.017) in the t_1 dimension and then zero filled in t_1 to give a 4K by 4K data matrix.

NOESY Experiments. Phase-sensitive proton NOESY experiments were recorded in D_2O solution at several mixing times (50−400 ms) and temperatures (2−30 °C) using a 5400-Hz sweep width in both dimensions. The transmitter frequency was set on the residual HOD resonance and irradiated with the decoupler channel during a 2.5-s relaxation delay. A steady-state pulse was applied at the beginning of the relaxation delay. A total of 4096 points were collected in the t_2 dimension, 512 t_1 values were collected for each data set, and 64 transients were collected for each t_1 value. The data were apodized with Gaussian functions in both dimensions (gf = 0.088; gf1 = 0.026) and zero filled in t_1 to give a 4K by 2K data matrix.

ROESY Experiments. Phase-sensitive proton ROESY experiments were recorded in D_2O solution with a spin lock time of 200 ms at 2, 10, and 20 °C using a 5400-Hz sweep width in both dimensions. The transmitter frequency was set on the residual HOD resonance and irradiated with low power using the transmitter during a 2.5-s relaxation delay.

A steady-state pulse was applied at the beginning of the relaxation delay. A total of 4096 points were collected in the t_2 dimension, 512 t_1 values were collected for each data set, and 64 transients were collected for each t_1 value. The data were apodized with Gaussian functions in both dimensions (gf = 0.112; gf1 = 0.017) and zero filled in t_1 to give a 4K by 2K data matrix.

TOCSY Experiments. TOCSY experiments were recorded in D_2O solution at several spin lock times (25−100 ms) and temperatures (2−30 °C) using a 5400-Hz sweep width in both dimensions. The transmitter frequency was set on the residual HOD resonance which was irradiated with low power using the transmitter during a 2.5-s relaxation delay. A trim pulse of 0.0002 s was used. A total of 4096 points were collected in the t_2 dimension, 512 t_1 values were collected for each data set, and 64 transients were collected for each t_1 value. The data were apodized with Gaussian functions in both dimensions (gf = 0.104; gf1 = 0.023) and zero filled in t_1 to give a 4K by 2K data matrix.

DQFCOSY Experiments. Phase-sensitive DQFCOSY experiments were recorded in D_2O solution at 2, 10, and 20 °C using a 5400-Hz sweep width in both dimensions. The transmitter frequency was set on the residual HOD resonance irradiated with low power using the transmitter during a 2.0-s relaxation delay. A total of 4096 points were collected in the t_2 dimension, 1024 t_1 values were collected for each data set, and 96 transients were collected for each t_1 value. The data were apodized with a shifted sine-bell function in the t_1 dimension (sb1 = −0.052; sbs1 = −0.019) and zero filled in t_1 to give a 4K by 2K data matrix.

Computational Studies. Energy minimization calculations were performed using Biosym Technologies Inc. molecular simulation program, Discover (version 2.9), employing the AMBER force field. Structures were displayed with the Biosym graphics program, Insight II (version 2.3.0). The partial charges for the modified guanine and the AF moiety were determined from a MOPAC calculation.

The restrained energy minimization calculations employed a flat-bottom potential to restrain the atom pair within a range of acceptable distances; when the distance, R_{ij}, between atoms i and j is within the lower (R_L) and upper (R_U) bounds, no energy penalty is added. The distance restraint penalty function consisted of a five-section continuous function:

$$E = \begin{cases} E_{L,max} + (R_{L,max} - R_{ij})F_{L,max} & R_{ij} < R_{L,max} \\ K_L(R_{ij} - R_L)^2 & R_{L,max} < R_{ij} \le R_L \\ 0 & R_L < R_{ij} \le R_U \\ K_U(R_{ij} - R_U)^2 & R_U < R_{ij} \le R_{U,max} \\ E_{U,max} + (R_{ij} - R_{U,max})F_{U,max} & R_{U,max} < R_{ij} \end{cases}$$

where R_L is the lower bound distance, R_U is the upper bound distance, R_{ij} is the current distance between the two atoms, $R_{L,max}$ is the maximum lower distance, and $R_{U,max}$ is the maximum upper bound distance. $F_{L,max}$, $F_{U,max}$, K_L, and K_U are force constants. The force constants K_L and K_U ranged from 20 to 100 kcal mol^{-1} Å^{-1}, and $F_{L,max}$, and $F_{U,max}$ were 1000 kcal mol^{-1} Å^{-1}. NMR-derived 2-aminofluorene to DNA interproton distances for the external-AF and inserted-AF conformations (see Results) and hydrogen-bonding restraints consisting of B-form DNA atom pair distances for each hydrogen bond in a G·C or A·T base pair as an upper bound distance restraint (G-O6 to C-N4H, 2.08 Å; G-N1H to C-N3, 1.99 Å; G-N2H to C-O2, 1.77 Å; T-O4 to A-N6H, 2.02 Å; T-N3H to A-N1, 1.88 Å) were employed.

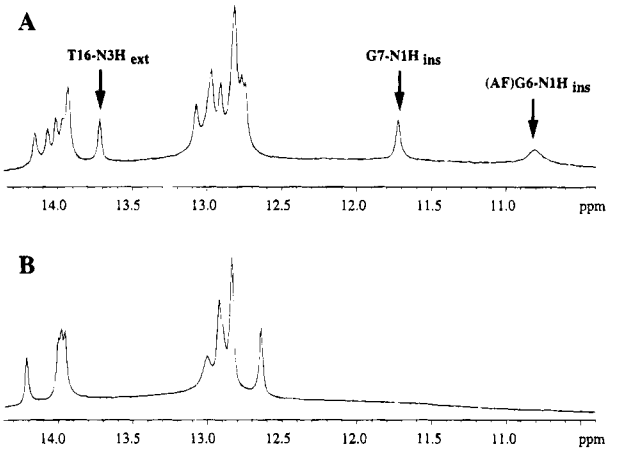

FIGURE 2: One-dimensional proton NMR spectrum of the imino proton region: (A) AF-10-mer duplex and (B) unmodified 10-mer duplex. Spectra were recorded at 10 °C in a 9:1 H_2O/D_2O buffer.

Energy minimization calculations were performed in the presence of sodium counterions and explicit solvent to adequately hydrate the portion of the AF-G6 residue that protrudes from the helix in each structure. Initial *in vacuo* calculations on the external-AF conformation employing a distance-dependent dielectric and reduced partial charges on the phosphate oxygens to mimic solvent were found to distort the helix and resulted in the distal protons (F-H5, F-H6, F-H7, and F-H8) of the AF moiety approaching the T13 and T12 base protons on the partner strand. The presence of explicit solvent in the energy minimization calculations prevented this distortion of the duplex and was consistent with the lack of observed NOEs in the NMR data between the distal fluorene protons and DNA protons. Solvation of the AF-modified DNA duplex was achieved by first placing sodium ions 3.5 Å from each phosphate at the bisector of the oxygen−phosphorus−oxygen angle. A cube, 3 Å larger than the DNA duplex and sodium counterions on each side, was then randomly filled with approximately 1000 water molecules from Insight II, and a periodic boundary condition was employed. The water was first energy minimized with the DNA and counterions in a fixed position, and then the entire solvated molecule was energy minimized. A nonbond cutoff distance of 15 Å was used with the Discover (version 2.9) switching function (fifth-order polynomial), employing a 1.5-Å range over which the function decreases from 1 to 0.

RESULTS

Chemical Exchange. The existence of two major conformations of the AF-10-mer duplex was apparent in both one-dimensional and two-dimensional NMR spectra. The observation of 16 identifiable resonances (Figure 2A) in the one-dimensional imino proton region of the spectrum (10−15 ppm) for the AF-10-mer contrasts with the 10 imino proton resonances observed for the unmodified 10-mer duplex (Figure 2B). Also, the broadening observed in the DNA base proton resonances when compared to the DNA base protons of the unmodified 10-mer duplex (Figure B, supplementary material) suggested the presence of slow chemical exchange. Chemical exchange cross-peaks were observed in NOESY spectra (Figure 3A and Figure C,

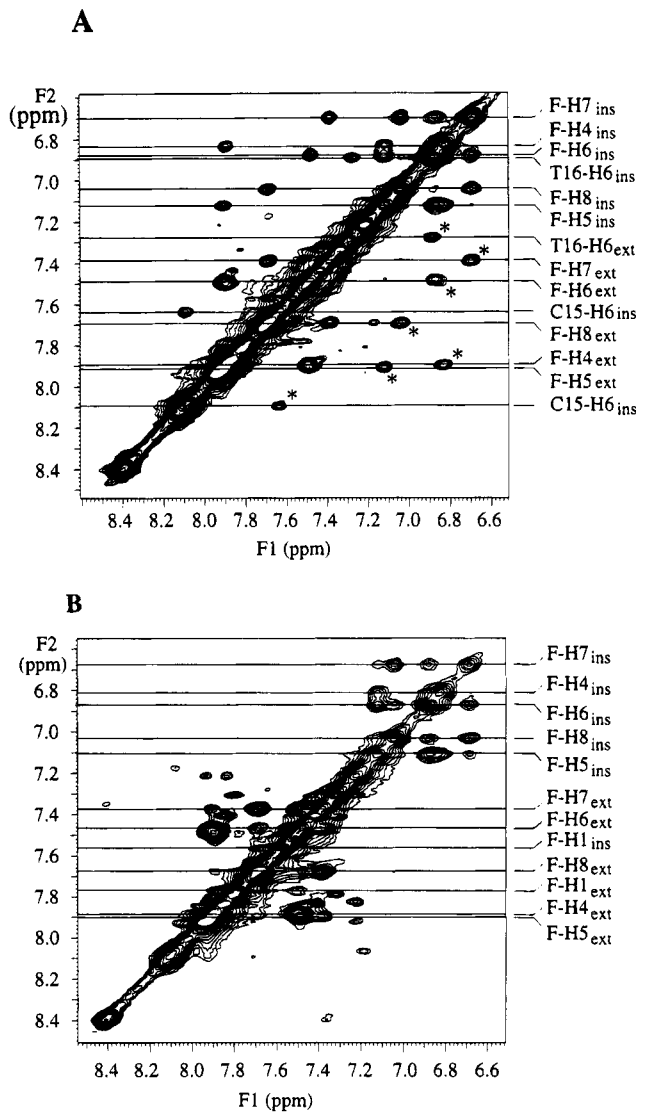

FIGURE 3: Portion (aromatic DNA base protons and fluorene protons) of a two-dimensional NOESY spectrum with a 100-ms mixing time in D_2O buffer. Proton resonances within each conformation are indicated by a subscript: ext and ins for external-AF conformation and inserted-AF conformation, respectively. Panels: (A) recorded at 10 °C; chemical exchange cross-peaks are labeled with an asterisk (*); (B) recorded at 2 °C; chemical exchange cross-peaks are absent or very weak.

supplementary material) and ROESY spectra (Figure D, supplementary material) recorded at 10, 20, and 30 °C. Examination of the chemical exchange cross-peak patterns indicated the presence of two conformations, referred to as the external-AF and inserted-AF conformations. The relative population of each conformation was determined by analysis of imino proton resonance intensities in spectra recorded at 10 °C (Figure 2A) and 2 °C for the well-resolved T16-N3H resonance in the external-AF conformation (13.7 ppm) and the G7-N1H resonance in the inserted-AF conformation (11.7 ppm). A comparison of resonance intensities, determined from integration of these imino proton resonances, indicates that the two conformers exist in approximately (±10%) equal population. The relative population of each conformer was also evaluated by comparing cross-peak volumes for protons with a fixed interproton distance (e.g., C-H5 to C-H6, T-H6 to T-CH3, F-H8 to F-H7, etc.) for each conformation in a 100 ms NOESY spectrum recorded at 2 and 20 °C. These data indicate an equal population (±10%) of each conformation at 20 °C, whereas at 2 °C the population ratio of the external-AF conformer to inserted-AF conformer was 60:40 (±10%).

Table 1: Chemical Shift Values of the 2-Aminofluorene Protons at 2 °C[a]

proton	external-AF conformation	inserted-AF conformation
F-H1	7.77	7.57
F-H3	n/a[b]	n/a[b]
F-H4	7.88	6.82
F-H5	7.89	7.11
F-H6	7.47	6.87
F-H7	7.38	6.67
F-H8	7.68	7.04
F-H9/9′	4.10, 4.04	3.40, 3.36

[a] Values given are in parts per million referenced to TSP at 0.0 ppm. [b] n/a = resonance not assigned.

An estimate of the chemical exchange lifetime was obtained by measuring chemical shift separations at 2 °C where the conformers are undergoing slow chemical exchange and then using these values at the coalescence temperature (Becker, 1980; Sandström, 1982). To reflect the complications in measuring the lifetime due to overlap of resonances and the lack of coalescence for many resonances even at 30 °C, we estimate that the chemical exchange lifetime is greater than 3 ms and less than 20 ms at 30 °C (Eckel & Krugh, 1994).

Two-dimensional NMR experiments were initially performed at 10, 20, and 30 °C with relatively narrow proton resonance line widths observed at 10 and 20 °C. Many assignments were made at these temperatures, although the assignment process was difficult and complete connectivities within each conformation could not be achieved due to the complications of chemical exchange. A subsequent observation that the exchange lifetime was longer than the mixing time at 2 °C facilitated the determination of individual resonance assignments for each conformation because NOESY spectra recorded at 2 °C did not exhibit chemical exchange cross-peaks for mixing times ≤200 ms (Figure 3B and Figure E, supplementary material) and only weak exchange cross-peaks at longer mixing times (400 ms).

Assignment of the 2-Aminofluorene Protons. Observed NOE interactions and chemical exchange cross-peaks in NOESY spectra (Figure 3A,B) and ROESY spectra (Figure D, supplementary material) and scalar coupling interactions in DQFCOSY spectra (Figure F, supplementary material) and TOCSY spectra (Figure G, supplementary material) at 20, 10, and 2 °C were used to establish individual assignments for the 2-aminofluorene protons in the external-AF and inserted-AF conformations (Table 1). The geminal F-H9/H9′ protons were identified by their characteristic upfield chemical shifts (3.36, 3.40 ppm for the inserted-AF conformation and 4.10, 4.04 ppm for the external-AF conformation at 2 °C). The F-H8 and F-H1 protons were subsequently assigned from NOE interactions with F-H9/H9′ protons (Figure 4A–C). The F-H5, F-H6, and F-H7 protons were assigned in DQFCOSY spectra (Figure F, supplementary material), and the F-H5, F-H6, F-H7, and F-H8 assignments were confirmed in NOESY spectra (Figure 3A,B) and TOCSY spectra (Figure G, supplementary material). The F-H4 proton was assigned from its NOESY (Figure 3A,B) and TOCSY (Figure G, supplementary material) cross-peaks to F-H5. The F-H3 proton was not assigned.

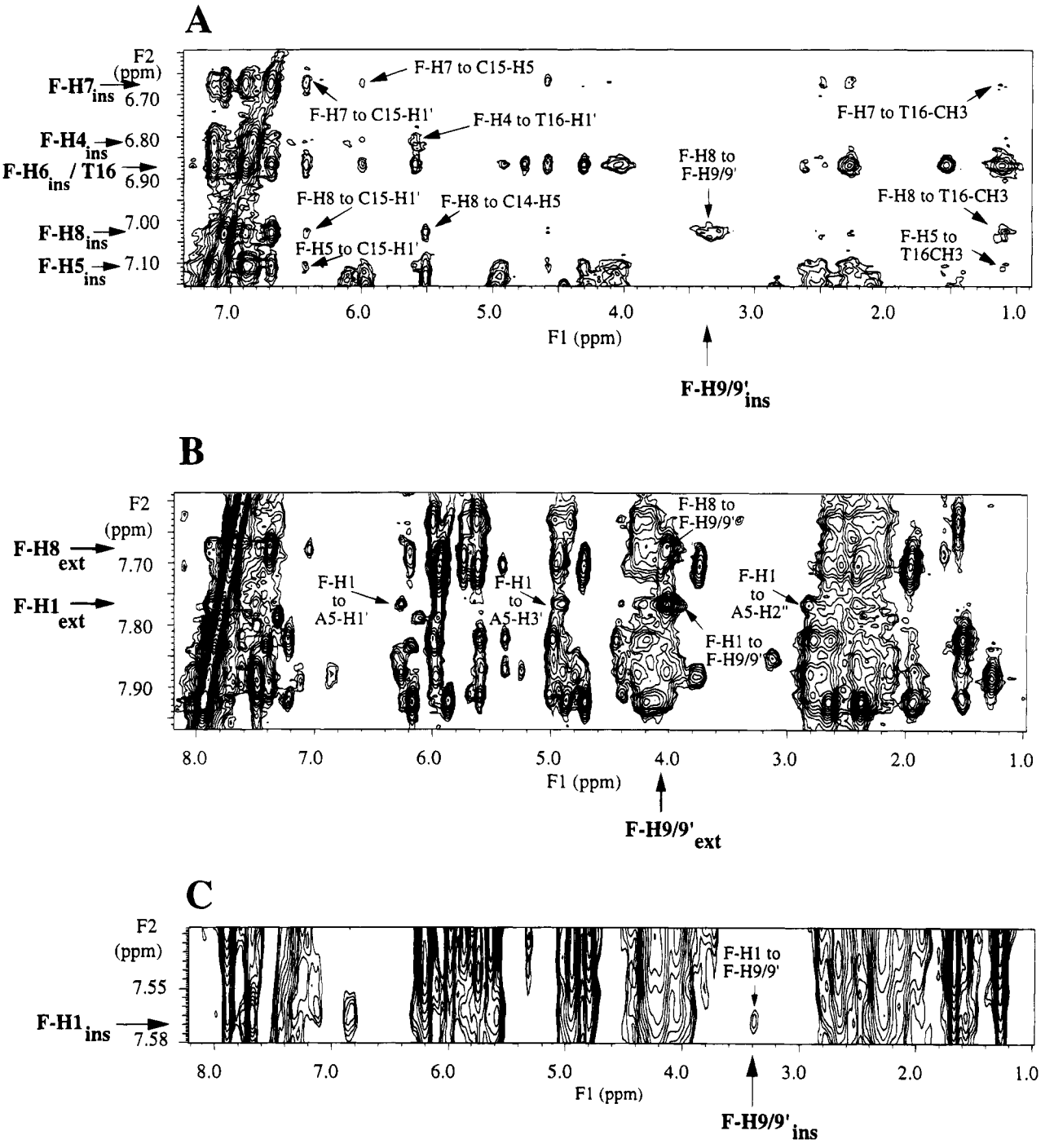

FIGURE 4: Portion of a two-dimensional NOESY spectrum at 2 °C with a 100-ms mixing time in D_2O buffer. Panels: (A) F-H8$_{ins}$ to F-H9/9'$_{ins}$ and AF to DNA NOE cross-peaks for the inserted-AF conformation are labeled; (B) F-H1$_{ext}$ to A5−H1'$_{ext}$, A5-H3'$_{ext}$, A5-H2"$_{ext}$, and F-H9/9'ext and F-H8$_{ext}$ to F-H9/9'$_{ext}$ NOE cross-peaks are labeled; (C) F-H1$_{ins}$ to F-H9/9'$_{ins}$ NOE cross-peak is labeled.

Fluorene proton resonances in NOESY spectra (Figure 3A,B), DQFCOSY spectra (Figure F, supplementary material), and TOCSY spectra (Figure G, supplementary material) were found as two groups of resonances (Table 1). The chemical shift values of the downfield F-H5, F-H6, F-H7, and F-H8 fluorene protons (7.4−7.9 ppm) were remarkably similar to chemical shift values for the corresponding fluorene protons of a dG-AAF monomer (Evans et al., 1986), which suggested a solvent-exposed location for the AF moiety. We designated this as the external-AF conformer to reflect the external location of the distal protons (F-H5, F-H6, F-H7, and F-H8) of the fluorene moiety. The fluorene F-H5, F-H6, F-H7, and F-H8 proton chemical shift values from the other conformer are significantly upfield (~0.6 ppm) from equivalent resonances in the external-AF conformer and are similar to chemical shift values observed in the AAF-9-mer where the fluorene moiety is stacked with adjacent bases (O'Handley et al., 1993). The second conformer was labeled the inserted-AF conformation to reflect the position of the fluorene moiety within the DNA duplex.

Assignment of DNA Protons. The presence of two sets of resonances, one from the inserted-AF conformation and one from the external-AF conformation, complicated DNA resonance assignments. NOEs between the fluorene protons and DNA protons in each conformation were used to differentiate the DNA proton resonances that were associated with the inserted-AF conformation from those of the external-

Table 2: Chemical Shift Values of the Exchangeable DNA Protons at 2 °C[a]

	external-AF conformation			
base pairs	G-N1H	T-N3H	C-N4H$_b$[b]	C-N4H$_{nb}$[c]
C1·G20	13.03		8.21	7.08
A2·T19		13.98		
C3·G18	12.79		8.01	6.59
C4·G17	12.83		8.46	6.90
A5·T16		13.76		
AF-G6·C15	13.07		8.80	6.95
G7·C14	12.76		8.58	7.11
A8·T13		14.00		
A9·T12		14.10		
C01·G11	12.80		8.43	6.70
	inserted-AF conformation			
base pairs	G-N1H	T-N3H	C-N4H$_b$[b]	C-N4H$_{nb}$[c]
C1·G20	13.03		8.21	7.08
A2·T19		13.98		
C3·G18	12.79		8.04	6.59
C4·G17	12.95		8.48	6.85
A5·T16		12.98		
AF-G6 C15	10.80		n/a[d]	n/a[d]
G7·C14	11.70		7.88	6.96, 6.80
A8·T13		13.95		
A9·T12		14.20		
C10·G11	12.80		8.43	6.70

[a] Values given in parts per million referenced to TSP at 0.0 ppm. [b] Hydrogen-bonded cytosine amino proton. [c] Non-hydrogen-bonded cytosine amino proton. [d] n/a = resonance not assigned.

AF conformation. The NOE interactions shown in Figure 4A between the fluorene protons of the inserted-AF conformer and the DNA base and sugar protons of the partner strand (G11−G20) established that these proton resonances were from the inserted-AF conformation. Subsequent sequential assignments from these resonances completed the assignment process for the G11−G20 resonances of the inserted-AF conformer. Thus, the remaining set of DNA proton resonances for the partner strand was associated with the external-AF conformation.

For the AF-modified strand (C1−C10), loss of the H8 proton of G6 upon AF modification interrupts the base proton to sugar proton connectivity path for the C1 to C10 strand; connectivities were established from C1 to A5 and G7 to C10 (see below). The F-H1 proton in the external-AF conformation has NOE interactions with the A5 sugar protons (Figure 4B), which provided the assignment of one set of C1 to A5 DNA protons of the AF-modified strand to the external-AF conformation. The two sets of DNA protons of G7 to C10 were differentiated by the assignment of an A8-H2 proton resonance to the inserted-AF conformation. A one-dimensional NOE experiment at 2 °C in H_2O (Eckel, 1994) exhibited an NOE from the G7-N1H imino proton at 11.7 ppm (inserted-AF conformation) to the adjacent T13-N3H imino proton at 13.95 ppm, which was used to assign the T13 imino proton resonance and its corresponding complementary A-H2 proton resonance of A8 to the inserted-AF conformation. This assignment allowed the differentiation of the G7-C10 base and sugar proton resonances of the inserted-AF and external-AF conformations.

Assignment of Exchangeable Nucleic Acid Protons. The exchangeable proton resonances were assigned (Table 2) by one-dimensional NOE experiments at 2 and 10 °C and by tracing interbase connectivities exclusively for each conformation within two-dimensional NOESY experiments at 2 °C using established approaches (Sklenar et al., 1987; Wemmer, 1992; Wüthrich, 1986). One-dimensional and two-dimensional NMR spectra of the imino proton region (10−15 ppm) exhibit 16 observable resonances for the AF-10-mer duplex (Figures 2A and 5). The C4·G17, A5·T16, AF-G6·C15, G7·C14, A8·T13, and A9·T12 imino protons were observed at two chemical shift positions and have been individually assigned to their specific conformations. The imino protons of the C1·G20, A2·T19, C3·G18, and C10·G11 base pairs were found at only one chemical shift.

Guanine imino protons (G7, G11, G17, G18, and G20) were assigned from observed interbase NOE interactions with their complementary cytosine hydrogen-bonded and non-hydrogen-bonded amino protons (Figure 5, cross-peaks a and a′, b and b′, c and c′, d and d′, e and e′, and f and f′). The cytosine amino protons also exhibited NOE interactions with their own H5 proton, and at long mixing times an NOE cross-peak could be observed between the complementary cytosine H5 proton and the guanine imino proton (Figure 5, cross-peaks a″, b″, d″, and e″). The H5 proton resonances for each cytosine (C1, C3, C4, C10, C14, and C15) in the external-AF and inserted-AF conformations were assigned from experiments in D_2O buffer at 2 °C and were used in the assignment of each guanine imino proton to the individual conformations. The G20-N1H and G11-N1H terminal imino proton resonances were broad and exhibited strong exchange cross-peaks to the H_2O resonance.

The AF-G6 imino proton for the external-AF conformation at 13.07 ppm was assigned from NOEs between it and the complementary C15 amino protons and the C15-H5 proton (Figure 5, cross-peaks g, g′, g″). This NOE pattern confirmed the presence of a Watson−Crick base pair. The AF-G6 imino proton resonance from the external-AF conformation (13.07 ppm) exhibited a chemical exchange peak at 10 °C to the resonance at 10.8 ppm (Figure H, supplementary material). Accordingly, this resonance was assigned to the AF-G6 imino proton for the inserted-AF conformer. The upfield-shifted AF-G6 imino proton resonance (10.8 ppm) exhibited no evidence of hydrogen bonding with its complementary cytosine (C15) and had a strong exchange cross-peak to the H_2O resonance.

Thymine imino protons (T12, T13, T16, and T19) were assigned from observed NOE interactions between the thymine imino and its complementary adenine H2 proton (Figure 5, cross-peaks h, i, j, k, l, m, and n). The adenine H2 protons were assigned from NOEs to the intraresidue H1′ and the 5′-neighboring H1′ sugar protons in D_2O solution (Table 3). In addition, coalescence of the inserted-AF and external-AF imino proton resonances for T12 and T13 observed as the temperature was increased (2−32 °C) in one-dimensional NMR experiments (Figure I, supplementary material) aided in deciphering the assignments of these overlapped resonances.

Assignment of Nonexchangeable Nucleic Acid Protons. DNA base proton and sugar proton resonances for the external-AF and inserted-AF conformations have been assigned by analysis of NOESY and TOCSY experiments at 2, 10, and 20 °C at pH 7.0 in D_2O using standard strategies for DNA oligomers (van de Ven & Hilbers, 1988; Wemmer, 1992; Wüthrich, 1986). The assignment process was complicated by the presence of chemical exchange which was manifested as the doubling or broadening of proton resonances, creating overlap of many resonances. Resonance assignments at 2 °C are given in Table 3.

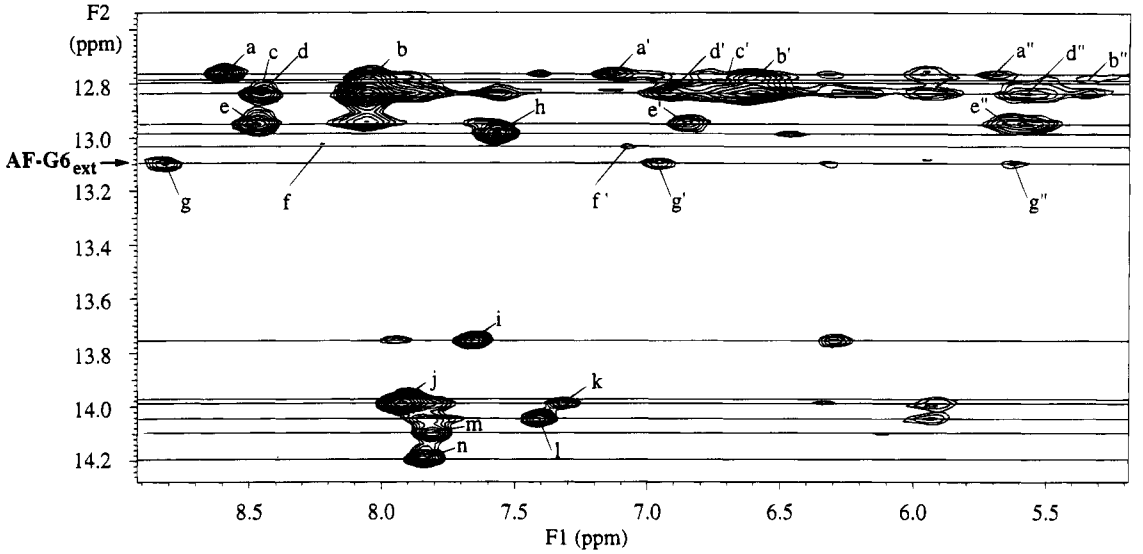

FIGURE 5: Portion of a two-dimensional NOESY spectrum at 2 °C with a 125-ms mixing time in H_2O buffer. Guanine imino proton to cytosine amino and H5 protons are shown for each G•C base pair, except for the upfield-shifted G7•C14 and AF-G6•C15 imino proton resonances for the inserted-AF conformation. Thymine imino proton to adenine H2 proton resonances for each A•T base pair are shown. Cross-peaks are labeled as follows: a, G7(N1H)$_{ext}$−C14(N4Hb)$_{ext}$; a′, G7(N1H)$_{ext}$−C14(N4H$_{nb}$)$_{ext}$; a″, G7(N1H)$_{ext}$−C14(CH5)$_{ext}$; b, G18-(N1H)−C3(N4H$_b$); b′, G18(N1H)−C3(N4H$_{nb}$); b″, G18(N1H)−C3(CH5); c, G11(N1H)−C10(N4H$_b$); c′, G11(N1H)−C10(N4H$_{nb}$); d, G17-(N1H)$_{ext}$−C4(N4H$_b$)$_{ext}$; d′, G17(N1H)$_{ext}$−C4(N4H$_{nb}$)$_{ext}$; d″, G17(N1H)$_{ext}$−C4(CH5)$_{ext}$; e, G17(N1H)$_{ins}$−C4(N4H$_b$)$_{ins}$; e′, G17(N1H)$_{ins}$−C4(N4H$_{nb}$)$_{ins}$; e″, G17(N1H)$_{ins}$−C4(CH5)$_{ins}$; f, G20(N1H)−C1(N4H$_b$); f′, G20(N1H)−C1(N4H$_{nb}$); g, AF-G6(N1H)$_{ext}$−C15(N4H$_b$)$_{ext}$; g′, AF-G6(N1H)$_{ext}$−C15(N4H$_{nb}$)$_{ext}$; g″, AF-G6(N1H)$_{ext}$−C15(CH5)$_{ext}$; h, T16(N3H)$_{ins}$−A5(H2)$_{ins}$; i, T19(N3H)−A2(H2); j, T16(N3H)$_{ext}$−A5(H2)$_{ext}$; k, T13(N3H)$_{ext}$−A8(H2)$_{ext}$; l, T13(N3H)$_{ins}$−A8(H2)$_{ins}$; m, T12(N3H)$_{ins}$−A9(H2)$_{ins}$; and n, T12(N3H)$_{ext}$−A9(H2)$_{ext}$.

Table 3: Chemical Shift Values of the Nonexchangeable DNA Protons at 2 °C[a]

	external-AF conformation					inserted-AF conformation				
base	H8/H6	H5/CH$_3$/H2	H1′	H2″/2′ [b]	H3′	H8/H6	H5/CH$_3$/H2	H1′	H2″/2′ [b]	H3′
C1	7.71	5.94	5.62	2.40/1.96	4.73	7.70	5.92	5.60	2.39/1.94	4.72
A2	8.40	7.92	6.25	2.92/2.81	5.05	8.38	7.91	6.23	2.91/2.80	5.04
C3	7.36	5.33	5.87	2.36/1.98	4.80	7.34	5.32	5.86	2.34/1.94	4.79
C4	7.41	5.57	5.24	2.12/1.92	4.71	7.52	5.63	5.31	2.26/2.11	4.80
A5	7.88	7.65	6.26	2.79/2.39	4.97	7.86	7.58	6.30	3.12/2.41	4.90
AF-G6			5.57	2.27/3.40	4.95			5.67	2.55/n/a[c]	5.00
G7	7.64		5.66	2.65/2.56	4.97	7.71		5.40	2.66/2.54	4.96
A8	8.12	7.40	6.03	2.93/2.68	5.08	8.09	7.30	5.98	2.92/2.67	4.99
A9	8.05	7.80	6.10	2.83/2.51	5.02	8.07	7.84	6.16	2.85/2.50	5.00
C10	7.18	4.99	5.96	2.12/2.10	4.99	7.21	4.98	5.98	2.12/2.10	4.98
G11	7.88		5.97	2.81/2.71	4.80	7.88		5.96	2.80/2.69	4.79
T12	7.51	1.27	6.20	2.66/2.26	4.94	7.48	1.24	6.17	2.64/2.23	4.92
T13	7.54	1.66	6.19	2.65/2.28	4.92	7.44	1.56	6.10	2.62/2.20	4.93
C14	7.69	5.74	5.88	2.56/2.20	4.86	7.14	5.50	5.96	2.50/2.27	4.94
C15	7.63	5.62	5.99	2.60/2.18	4.82	8.10	6.28	6.42	2.62/2.32	4.90
T16	7.28	1.54	5.68	2.29/1.89	4.84	6.87	1.10	5.58	2.28/1.53	4.75
G17	7.91		5.60	2.80/2.78	5.00	7.87		5.38	2.70/2.55	4.96
G18	7.83		5.98	2.77/2.63	4.98	7.82		6.00	2.77/2.61	4.97
T19	7.22	1.48	5.86	2.37/1.94	4.87	7.21	1.50	5.86	2.37/1.92	4.86
G20	7.93		6.16	2.65/2.41	4.71	7.92		6.18	2.64/2.40	4.70

[a] Values given are in parts per million referenced to TSP at 0.0 ppm. [b] Differentiation of H2″ and H2′ established by the relative intensities of the H1′ to H2″ and H1′ to H2″ cross-peaks in the 100-ms NOESY spectrum. Verification with scalar coupling patterns was not possible due to line broadening; therefore, some assignments may be reversed. [c] n/a = resonance not assigned.

The base proton to H1′ sugar proton NOE connectivities of the AF-modified strand in both conformations at 2 °C could be traced from C1 to A5 and from G7 to C10 (Figure 6A). The interruption in the connectivities was due to the loss of the H8 proton of G6 upon covalent attachment of the AF moiety at this position (Figure 1). The base to H1′ sugar proton NOE connectivities of the partner strand were traced from G11 to G20 for both conformations at 2 °C (Figure 6B). The base proton assignments were confirmed by tracing connectivities in the base proton to H2′/H2″ sugar proton and H3′ sugar proton regions. DNA sugar proton assignments were confirmed by TOCSY experiments. The H2′ and H2″ resonances were differentiated by the relative intensities of the H1′ to H2′ and H1′ to H2″ cross-peaks in the 100-ms NOESY spectrum; the H1′ to H2″ NOE interactions exhibit stronger cross-peaks than the H1′ to H2′ NOE interactions in all sugar conformations. Attempts to use a DQFCOSY experiment to differentiate the H2′ and H2″ protons by their coupling patterns with the H1′ proton were unsuccessful due to the broad H2′/H2″ proton resonances creating cancellation of the phase-sensitive coupling patterns of the cross-peaks, thus eliminating the observed signal. The adenine H2 protons were located from inversion−recovery (T_1) experiments at 2 and 10 °C in which A-H2 proton resonances were differentiated by their long spin−lattice relaxation times (Figure J, supplementary mate-

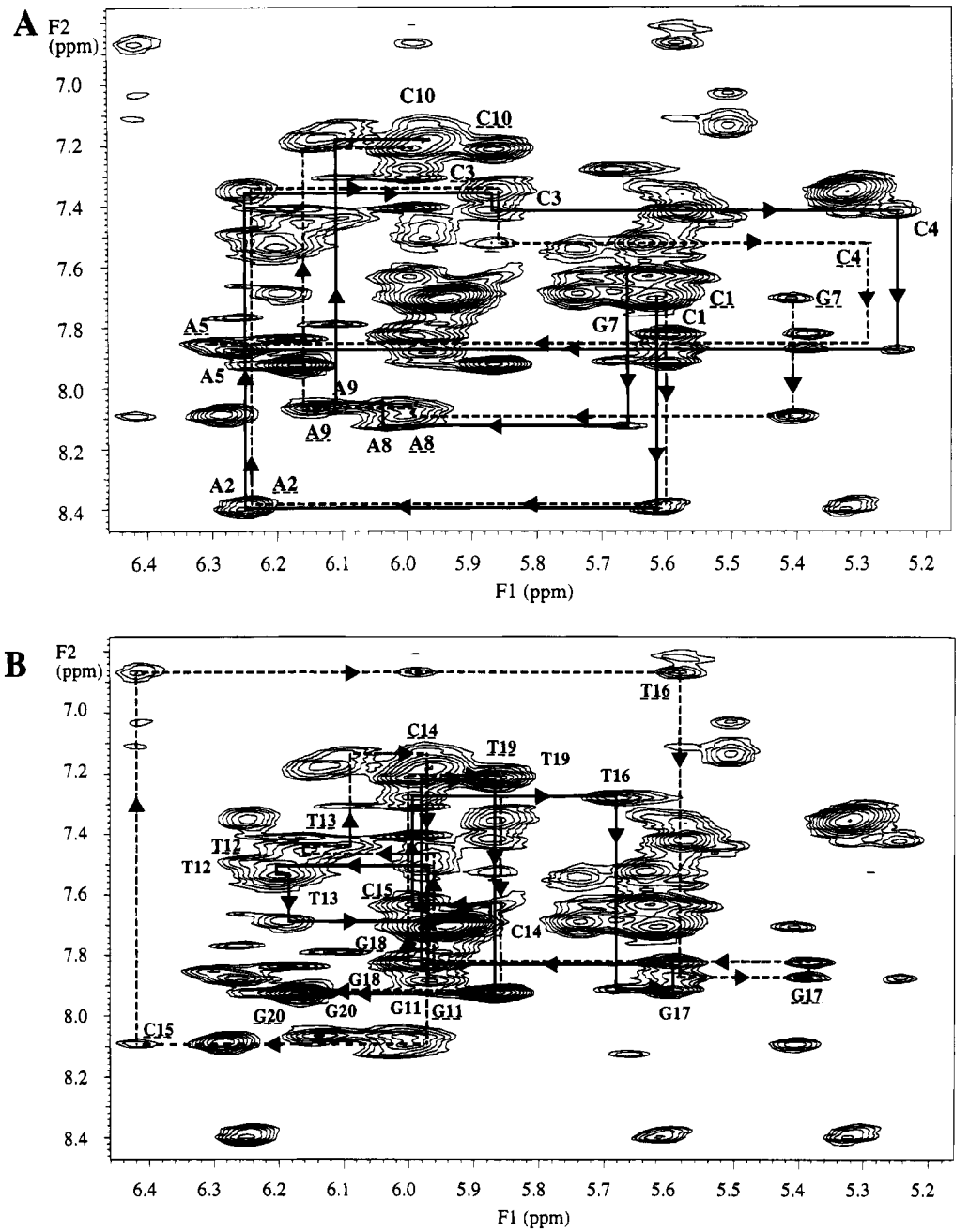

FIGURE 6: Portion of a two-dimensional NOESY spectrum at 2 °C with a 200-ms mixing time in D_2O buffer. Panels: (A) sequential connectivities of the AF-modified strand, d(C1-A2-C3-C4-A5-{AF-G6}-G7-A8-A9-C10); (B) sequential connectivities of the partner strand, d(G11-T12-T13-C14-C15-T16-G17-G18-T19-G20). The sequential connectivities of the aromatic base protons (H8/H6) to the following DNA H1′ sugar proton are traced with solid lines for the external-AF conformation and with dashed lines for the inserted-AF conformation. Labels for the intranucleotide base to H1′ NOE cross-peaks (C1, A2, C3, etc.) are indicated with dashed underscores for NOE cross-peaks from the inserted-AF conformation.

rial) and assigned from observed NOE interactions with their own sugar H1′ and their 5′-neighboring sugar H1′ protons in D_2O experiments and from NOEs with their complementary thymine imino protons in H_2O solution.

For the inserted-AF conformation, the C4-H6 to C4-H1′ cross-peak was very weak but observable, while the C4-H1′ to A5-H8 NOE connectivity was not observed in the 200-ms mixing time NOESY spectrum (Figure 6A). The assignment of the A5-H8 proton resonance for the inserted-AF conformation was established by C4-H2′/H2″ to A5-H8 connectivities. The AF-G6 sugar protons for the external-AF and inserted-AF conformations were assigned from NOE and scalar coupling interactions among one another and NOE interactions with the neighboring G7-H8 base proton observed at 20, 10, and 2 °C; loss of the H8 proton on the AF-G6 residue eliminates the possibility of intranucleotide base to sugar NOEs. An unusually downfield-shifted H2′ resonance ($\Delta\delta = -0.90$ ppm) was observed for the external-AF conformation.

The glycosidic torsion angles for all of the DNA bases of both conformers (except AF-G6 which lacks an H8 base proton) were determined to be in an *anti* domain, as depicted by the larger relative magnitude of the H8/H6 to H2′ NOEs when compared to the H8/H6 to H1′ NOEs. Both the external-AF and inserted-AF conformations also exhibited NOE connectivity patterns that are characteristic of right-handed B-form DNA and, except for the AF-G6 and C15 bases in the inserted-AF conformer, are Watson–Crick base paired as discussed above.

Table 4: NMR-Derived Distance Restraints Used in Energy Minimization Calculations[a]

atom pair	calcd distance, Å	distance restraint, Å	obsd distance, Å
Inserted-AF Conformation			
F-H8 to C14-H5	3.0	3.0 ± 0.6	3.4
F-H7 to C15-H5	3.6	3.6 ± 0.7	4.0
F-H5 to C15-H1′	3.9	3.9 ± 0.8	4.4
F-H7 to C15-H1′	3.0	3.0 ± 0.6	2.8
F-H8 to C15-H1′	3.4	3.4 ± 0.7	3.9
F-H5 to T16-CH3	3.2	3.2 ± 0.6	3.6
F-H7 to T16-CH3	3.2	3.2 ± 0.6	3.4
F-H8 to T16-CH3	2.8	2.8 ± 0.6	2.6
F-H4 to T16-H1′	3.1	3.1 ± 0.6	3.3
External-AF Conformation			
F-H1 to A5-H1′	3.7	3.7 ± 0.7	4.4
F-H1 to A5-H2″	3.1	3.1 ± 0.6	2.4
F-H1 to A5-H3′	3.1	3.1 ± 0.6	3.3

[a] Cross-peak volumes from a 100-ms mixing time NOESY spectrum at 2 °C were used to calculate the atom pair distances for the external-AF and inserted-AF conformations. These calculated distances were used as distance restraints in restrained energy minimization calculations employing a flat-bottom potential to restrain the atom pair. Observed distances are measured from the final external-AF and inserted-AF structures shown in Figure 7.

NMR Distance Restraints. 2-Aminofluorene to DNA interproton distances for the external-AF and inserted-AF conformations were determined by measuring the cross-peak volumes from a 100-ms mixing time NOESY spectrum at 2 °C (Figure 4A,B) and calculating the sixth root ratio to an average C-H5 to C-H6 cross-peak volume (Eckel, 1994) where the vicinal protons have a fixed distance of 2.45 Å (Clore & Gronenborn, 1985; van de Ven & Hilbers, 1988; Wemmer, 1992). These calculated distances (Table 4) were employed as distance restraints (±20% for upper and lower bounds) in restrained energy minimization calculations. Observed 2-aminofluorene to DNA cross-peaks that exhibited overlap with other resonances (e.g., F-H6 to C15-H1′ and F-H6 to T16-CH_3 for the inserted-AF conformer) or extensive broadening at 2 °C (e.g., F-H1 to A5-H2′ for the external-AF conformer) were not used as distance restraints due to the difficulty in obtaining accurate cross-peak volume measurements for these resonances. Hydrogen-bonding restraints consisting of B-form DNA atom pair distances for each hydrogen bond in a G·C or A·T base pair (see Materials and Methods) were also employed for all 10 base pairs in the external-AF conformation and for 9 out of 10 base pairs in the inserted-AF conformation, consistent with the NMR data.

Initial Structures for Energy Minimization Calculations. The initial structure used for energy minimization of the external-AF conformer was right-handed B-form DNA (generated with Insight II) to which an AF moiety was attached at the C8 position of G6 to form an AF-G6 residue (Figure 1) with its glycosidic torsion angle in the *anti* domain. Maintenance of Watson–Crick base pairing for the AF-G6 and C15 bases, as determined from NMR data, placed the AF moiety in the major groove. The orientation of the AF moiety within the major groove for the external-AF conformation was not well-defined by the NMR data (only NOE interactions between F-H1 and A5 sugar protons were observed), so the AF moiety was rotated by 90° along the (AF)N2–(AF)C2 bond to obtain four starting structures for the restrained energy minimization calculations to determine if more than one AF position could satisfy the NMR distance restraints.

To generate an initial structure for energy minimization of the inserted-AF conformer, we used the starting structure of the external-AF conformer and positioned the AF moiety within the DNA duplex using the 2-aminofluorene to DNA distance restraints as a guide. Several observed NOEs (Figure 4A) between C14 and T16 base protons and fluorene protons show that the fluorene ring is located between the A5·T16 and G7·C14 base pairs. In addition, an F-H4 to T16-H1′ NOE interaction oriented the fluorene moiety close to the sugar–phosphate backbone of the partner strand.

In the inserted-AF conformer, 2-aminofluorene to DNA NOE interactions defined the stacked position of the AF moiety, but the locations of the modified guanine and the complementary cytosine were not as well characterized by the NOE data. Neither the imino proton nor the amino protons of the modified guanine exhibited any observable interactions with neighboring base or sugar protons to help define its location. Two locations of the AF-G6 base were employed in the energy minimization calculations for the inserted-AF conformer, and we refer to these as the *anti* and *syn* inserted-AF conformers. Conceptually, the *anti* conformer is generated by moving (by means of bond rotations) the AF-G6 residue so that the guanine base goes into the minor groove while the fluorene moiety stacks on adjacent base pairs. The glycosidic angle of the AF-G residue remains in the *anti* domain. To generate the series that we label as *syn* conformers, the AF-G6 residue was initially rotated by 180° about the glycosidic bond to place the guanine in a *syn* domain. The *syn* starting structure is generated by moving the fluorene moiety to a stacked position between the adjacent base pairs, which places the modified G6 base in the major groove. The complementary cytosine (C15) was positioned in both the major and the minor grooves of the duplex in the *anti* inserted-AF starting structures to determine which position was consistent with observed NMR data (i.e., a C15-H5 to F-H7 NOE interaction).

Energy Minimization Calculations. Restrained energy minimization calculations with explicit solvent were performed on the external-AF and inserted-AF starting structures using the calculated 2-aminofluorene to DNA NMR distance restraints and hydrogen-bonding restraints (see Materials and Methods). After the first round of energy minimization, the 2-aminofluorene to DNA NMR distance restraints were released, and energy minimization was continued using only the hydrogen-bonding restraints. Finally, the hydrogen-bonding restraints were released, and unrestrained energy minimization was performed. Only minor changes in the structures for the external-AF and inserted-AF conformations were observed after release of the restraints.

Energy-Minimized Structures. For the external-AF conformation, the lowest energy structure that satisfied distance restraints between the 2-aminofluorene and DNA protons (Table 4) had the AF moiety in the major groove with the modified guanine and its complementary cytosine as a Watson–Crick base pair, as required by the NMR data. In this structure (Figure 7, top), the AF moiety protrudes from the major groove with the F-H1–F-H8 side of the fluorene moiety pointing toward the 5′ end of the AF-modified strand. This energy-minimized structure is considered to be a reasonable representation of the external-AF conformation and is consistent with observed NMR data. However, energy minimization searches identified other possible external-AF structures of similar energies with slightly different orientations of the AF moiety that also satisfied the NMR distance

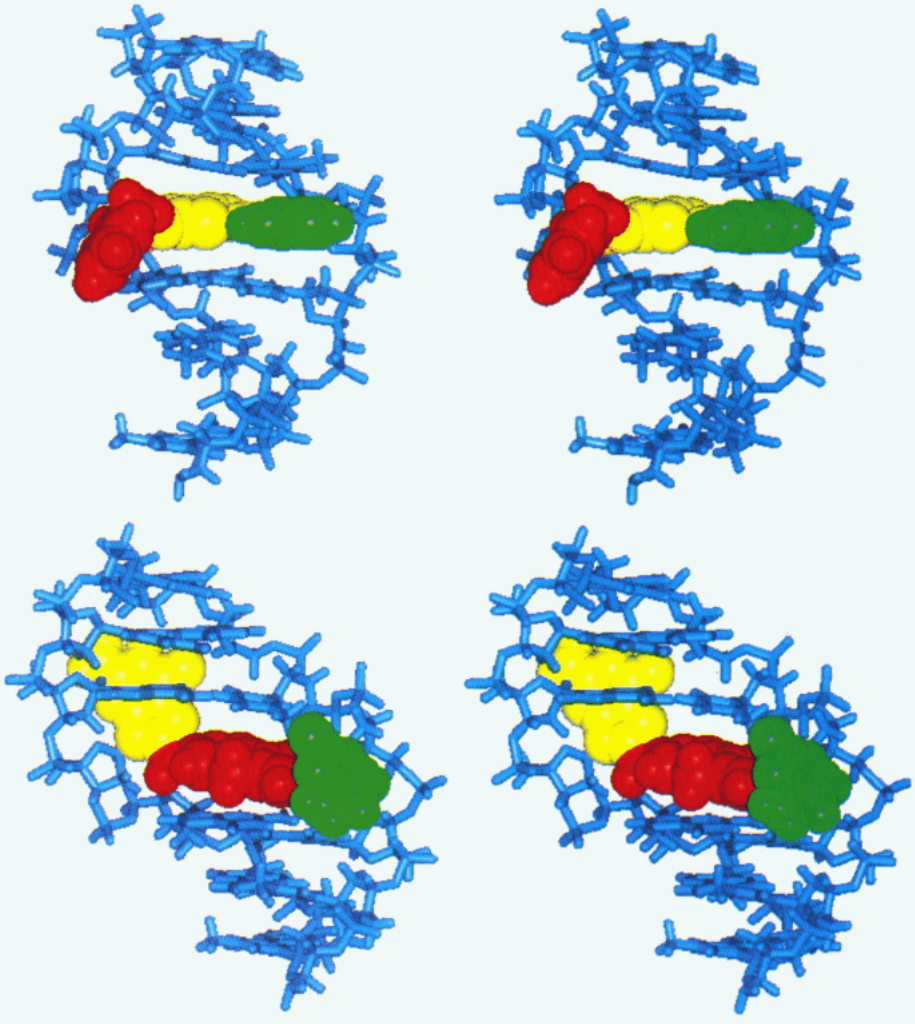

FIGURE 7: Stereoview of the energy-minimized conformations of the AF-modified duplex as viewed from the major groove in (top) the external-AF conformation and (bottom) the inserted-AF conformation. The seven-base portion of the duplex, d(A3−C4-A5-{AF-G6}-G7-A8-A9)·d(T12-T13-C14-C15-T16-G17-G18), is shown with the 2-aminofluorene moiety in red, the modified guanine in yellow, and the complementary cytosine in green.

restraints. The most important features of the external-AF structure as shown in Figure 7 (i.e., the AF moiety protrudes from the major groove and the AF-G6·C15 exists as a Watson−Crick base pair) were found in all low-energy external-AF structures.

For the inserted-AF conformation, the lowest energy structure that satisfied the distance restraints between the 2-aminofluorene and DNA protons (Table 4) had the inserted-AF moiety stacked between T16 and C14 with the modified guanine located in the minor groove and the complementary cytosine (C15) unstacked in the major groove (Figure 7, bottom). The orientation of the fluorene ring is well-defined by the NOEs between the fluorene protons and DNA base and sugar protons of the partner strand (Table 4). Displacement of the C15 into the minor groove failed to locate low-energy structures in which the C15-H5 to F-H7 NMR distance restraint was satisfied, and thus we believe C15 is unstacked in the major groove.

The possibility that the AF-G moiety may be in a *syn* conformation was also explored, and we located an energy-minimized conformer that had a *syn* AF-G that satisfied the NMR restraints (Figure K, supplementary material). For reasons presented below, we do not believe this structure is present to any significant extent. Although both *syn* and *anti* domain energy-minimized structures were located, the major structural feature of the inserted-AF conformation, namely, that the fluorene ring stacks between adjacent base pairs with denaturation of the AF-G6·C15 base pair, is well-defined by the NMR data and is observed in both structures (Figure 7, bottom, and Figure K, supplementary material).

DISCUSSION

Structural Features. Although the important features of the external-AF and inserted-AF conformers are clearly defined by the NMR data, the detailed structure of the duplex is not as well-defined. We chose not to include DNA base to sugar NOE restraints because similar chemical shifts of many resonances in the two conformers resulted in overlap of cross-peaks (e.g., see Figure 6), hindering the accurate measurement of many cross-peak volumes for determination of interproton distances. The need to record NOESY data at 2 °C to minimize chemical exchange also exacerbated the overlap of proton resonances due to the increased line broadening observed at low temperatures for all DNA oligomers. Although energy minimization provides detailed three-dimensional structures, we focus our attention on the location of the fluorene moiety and the base pairing of the modified guanine.

External-AF Conformation. The external-AF conformer of the AF-modified duplex exists as a relatively unperturbed right-handed B-form DNA duplex, with the AF-G6·C15 base pair intact and the AF moiety protruding from the major

groove of the duplex. A comparison of chemical shifts for both exchangeable and nonexchangeable DNA protons in the external-AF conformer with those from the unmodified duplex reveals only nominal chemical shift differences (except for the AF-G6 H2′ proton), consistent with minimal perturbation of the DNA duplex upon formation of the external-AF adduct (Eckel, 1994). A large downfield chemical shift difference (−0.90 ppm) is observed for the AF-G6 H2′ proton in the external-AF conformation that we ascribe to deshielding by the fluorene moiety. This large chemical shift difference is comparable to the downfield chemical shift values reported for the H2′ proton of the modified guanine in a *syn* dG-AAF (Evans et al., 1980) and a *syn* AF-G 11-mer duplex (Norman et al., 1989) in which deshielding of the H2′ proton is attributed to the guanine base in a *syn* conformation. Thus, it appears that either the AF moiety or a guanine base located in the major groove may result in deshielding of the H2′ proton of the modified guanine.

The loss of the guanine H8 proton upon formation of the AF-G6 adduct (Figure 1) precludes the use of this proton to determine the glycosidic angle of the AF-G6 base. However, the 2-aminofluorene to DNA distance restraints for the external-AF conformation are not satisfied if the AF-G6 residue is rotated to the *syn* domain. The external, protruding location of the AF moiety within the major groove of a relatively undistorted B-form DNA duplex (Figure 7, top) is consistent with DNA base to sugar connectivity patterns and cross-peak intensities, 2-aminofluorene to DNA NOE interactions, chemical shift values of the fluorene protons, and the lack of observed short distances between the distal fluorene protons and DNA protons.

The structure of the external-AF conformer is similar to models previously proposed for 2-aminofluorene-modified DNA oligomers. Evans (1980) determined from one-dimensional NMR experiments that the glycosidic torsion angle of dG-AF was preferentially in the *anti* domain and subsequently proposed a structure in which the AF moiety could reside in the major groove of an undistorted DNA duplex with the modified guanine in an *anti* conformation. Broyde and Hingerty (1983) employed minimized potential energy calculations on an AF-modified dCpdG dimer which identified a low-energy conformer with the fluorene moiety residing in the major groove of an undistorted B-type DNA helix. Thus, the NMR-derived energy-minimized structure for the external-AF conformer is consistent with the main features of previous models.

Inserted-AF Conformation. The inserted-AF conformation of the AF-modified duplex has the AF moiety stacked within the duplex, disrupting Watson−Crick base pairing between AF-G6 and C15 by displacing the modified guanine into the minor groove and the complementary cytosine into the major groove (Figure 7, bottom). Several observed NOEs between C14 and T16 base protons and fluorene protons (Table 4) delineate the stacked location of the fluorene moiety between the A5•T16 and G7•C14 base pairs. An F-H4 to T16-H1′ NOE interaction indicates that the F-H4−F-H5 side of the fluorene moiety is close to the partner strand. The inserted location of the fluorene residue is consistent with the shielding of the adjacent imino and base protons, T16-N3H ($\Delta\delta$ = +0.97 ppm), G7-N1H ($\Delta\delta$ = +0.85 ppm), C14-H6 ($\Delta\delta$ = +0.49 ppm), and T16-H6 ($\Delta\delta$ = +0.46 ppm), and the upfield chemical shift values of the fluorene protons for the inserted-AF conformer (Table 1).

The F-H7 to C15-H5 NOE interaction and deshielding of the C15-H6 ($\Delta\delta$ = −0.53 ppm) and C15-H5 ($\Delta\delta$ = −0.67 ppm) base protons are consistent with the displacement of the complementary base (C15) into an unstacked position in the major groove. The extrahelical location of the cytosine is not surprising since cytosine has been shown to form looped-out complexes (Kalnik et al., 1990; Morden et al., 1983; Zhou & Vogel, 1993), although in one case the extrahelical cytosine shifted to a stacked conformation at elevated temperatures (Kalnik et al., 1990).

The external-AF and inserted-AF conformers interconvert readily at 30 °C (~10-ms lifetime), and we use this to propose that the glycosidic torsion angle of the AF-G6 residue for the inserted-AF conformer is retained in an *anti* domain upon interconversion. It seems less likely that the bulky AF-G residue (Figure 1) would be able to find a path to rotate into a *syn* conformation on this time scale. Retaining the AF-G in the *anti* domain allows an interconversion path that has the guanine rotate into the minor groove while simultaneously moving the fluorene moiety from the major groove to a stacked position between the adjacent base pairs. However, we explored conformations in which the AF-G6 moiety was in the *syn* domain and identified energy-minimized structures that satisfy the distance restraints for the inserted-AF conformer given in Table 4 (a representative structure is shown in Figure K, supplementary material). Although the *syn* conformer satisfies the distance restraints, we do not believe that it is present in solution because the interchange between a *syn* inserted-AF conformer and the *anti* external-AF conformer would require the rotation of the bulky AF-G6 residue from an *anti* to a *syn* conformation.

The observation of the AF-G6 imino proton resonance at 20 °C (Figure I, supplementary material) for the inserted-AF conformer suggests that this imino proton is partially shielded from exchange with solvent and offers support for the *anti* inserted-AF conformation because in this conformer the modified guanine is in the minor groove with the imino proton partially protected by the backbone of the partner strand (Figure 7, bottom). In the *syn* inserted-AF conformer, the modified guanine is located in the major groove (Figure K, supplementary material), and the AF-G6 imino proton is in a more solvent-exposed location. In addition, the large downfield chemical shift (−0.32 ppm) observed for the A5-H2″ proton resonance in the inserted-AF conformer is presumably due to the deshielding of the resonance by the modified guanine in the minor groove, also offering support for the *anti* inserted-AF conformer.

It was important to consider the possibility of a *syn* inserted-AF conformer in addition to an *anti* inserted-AF conformer because previous theoretical and experimental studies have demonstrated the existence of both *anti* and *syn* AF-G conformers (Broyde & Hingerty, 1983; Cho et al., 1994; Evans et al., 1980; Hingerty & Broyde, 1986; Leng et al., 1980; Lipkowitz et al., 1982; Norman et al., 1989; Santella et al., 1980; van Houte et al., 1988, 1991). The conformations observed are determined by the stacking, electrostatics, hydrogen-bonding, hydrophobic, and van der Waals interactions within the system. It is intriguing that the two, structurally distinct conformers (external-AF and inserted-AF) of the AF-10-mer duplex have nearly the same overall free energies as indicated by the approximately equal populations observed in the NMR spectra. We expect, therefore, that the conformation of AF-modified DNAs will

be dependent both on the base opposite the AF-G residue and on the sequence of adjacent base pairs.

Possible Biological Implications. The existence of two interchangeable conformations may aid in understanding the biological diversity observed upon formation of AF adducts. Lesions induced by AF have been shown to be correctly bypassed by replication enzymes (Lutgerink et al., 1985; Michaels et al., 1991; Shibutani & Grollman, 1993; van de Poll et al., 1992), resistant to enzymatic repair in the cell (Gupta & Dighe, 1984; Poirier et al., 1982), and an inefficient block to replication enzymes (Fuchs & Seeberg, 1984; Tang et al., 1982). The external-AF conformation in which AF modification does not distort the right-handed B-type duplex, retaining Watson–Crick base pairing of the AF-modified guanine, is consistent with the ability of replication enzymes to bypass the lesion site and correctly incorporate cytosine opposite an AF-G adduct. Lack of distortion upon AF modification in the external-AF conformation also may allow the lesion to be inefficiently recognized by repair mechanisms in the cell (Fuchs & Seeberg, 1984).

AF-DNA lesions have also been shown to induce base substitutions and frame-shift mutations (Bichara & Fuchs, 1985; Carothers et al., 1993; Mah et al., 1989; Reid et al., 1990). The inserted-AF conformer in which Watson–Crick base pairing is disrupted may represent an AF lesion in a premutagenic conformation. Conformations of AF-modified DNA (Broyde & Hingerty, 1983; Norman et al., 1989; van Houte et al., 1987) and AAF-modified DNA (Broyde & Hingerty, 1987; Fuchs & Daune, 1972; Grunberger et al., 1970; O'Handley et al., 1993), in which the fluorene moiety is inserted, have previously been suggested to induce base substitution or frame-shift mutations due to a disruption of base pairing. The stacked location of the fluorene moiety in the inserted-AF conformer (Figure 7, bottom) and the AAF-9-mer (O'Handley et al., 1993) creates a loss of Watson–Crick base pairing by displacing the modified guanine and complementary cytosine. The resulting extrahelical position of the complementary cytosine suggests that the elimination of the partner C (−1 deletion) may enhance the stacking of the fluorene ring with the adjacent bases.

The AF- and AAF-modified DNA oligomers provide excellent model systems for studying −1 and −2 deletion mutations and are easily constructed by combining the modified strand with a shorter partner strand in which one or two bases opposite the modified guanine have been deleted. Fuchs and co-workers (Garcia et al., 1993) showed that an AAF-modified 14:13 heteroduplex exhibited enhanced thermal stability relative to the AAF-modified 14:14 homoduplex. Romano and Zhou (1993) constructed a model for a −2 deletion containing a C{AAF-G}C sequence incorporated into a 12:10 heteroduplex that exhibited the same T_m as the AAF-modified 12:12 homoduplex. We (Bailey, Guckian, and Krugh, in preparation) have obtained similar stability results for AAF −1 and −2 deletion models and have preliminary data that suggest the sequence context at the modification site is important. We have characterized the structure of the AAF −1 deletion model by two-dimensional NMR and have determined that the fluorene moiety is stacked within the duplex.

Understanding the relationship between structure and mutagenesis has long been a goal, as can be seen in the four decades of interest on the tautomerism of bases [e.g., see the commentary by Morgan (1993)] or an earlier article from the author's laboratory (Krugh, 1973). The facile interconversion between the structurally distinct external-AF and inserted-AF conformers may allow DNA replication enzymes that encounter the AF-G residue in an inserted position at the replication fork to pause until the appropriate conformation for recognition is obtained. We recognize, however, that the absence of replication enzymes and other replication machinery limits the interpretation of the present results in terms of mutagenesis. Finally, the nature of the complementary base (including deletions) and the effects of neighboring base pairs on the conformation and dynamics of AF-modified oligomers are areas of ongoing interest.

ACKNOWLEDGMENT

We thank our colleagues, Charles Bailey and Matthew Fountain, and Professor Suse Broyde (New York University) for many helpful discussions.

SUPPLEMENTARY MATERIAL AVAILABLE

Figures showing the HPLC chromatogram of the d(CAC-CAGGAAC)/AAAF reaction mixture (Figure A), the base proton region of a one-dimensional NMR spectrum recorded at 10 °C for the AF-10-mer and unmodified 10-mer (Figure B), the chemical exchange cross-peaks in the imino proton to imino proton region of a NOESY spectrum recorded at 10 °C in H_2O with a mixing time of 100 ms (Figure C), chemical exchange cross-peaks in the aromatic base proton and fluorene proton region of a ROESY spectrum recorded at 10 °C with a mixing time of 200 ms (Figure D), the imino proton to imino proton region of a NOESY spectrum recorded at 2 °C in H_2O with a mixing time of 100 ms (Figure E), the aromatic base proton and fluorene proton region of a DQFCOSY spectrum recorded at 10 °C (Figure F), the aromatic base proton and fluorene proton region of a TOCSY spectrum recorded at 20 °C in D_2O with a mixing time of 70 ms (Figure G), the one-dimensional NOE experiment at 10 °C showing the chemical exchange cross-peak for the (AF)G6–N1H proton (Figure H), the one-dimensional imino proton spectra recorded at 11–50 °C (Figure I), the base proton region of a one-dimensional inversion–recovery (T_1) experiment (Figure J), and a stereoview of an energy-minimized inserted-AF conformation with the AF-G6 glycosidic torsion angle in a *syn* domain (Figure K) (13 pages). Ordering information is given on any current masthead page.

REFERENCES

Becker, E. D. (1980) *High Resolution NMR: Theory and Chemical Applications*, Academic Press, New York.

Beland, F. A., & Poirier, M. C. (1989) in *DNA Adducts and Carcinogenesis* (Sirica, A. E., Ed.) pp 57–80, Plenum Press, New York.

Beland, F. A., & Kadlubar, F. F. (1990) in *Metabolic Activation and DNA Adducts of Aromatic Amines and Nitroaromatic Hydrocarbons* (Cooper, C. S., & Grover, P. L., Eds.) pp 267–325, Springer-Verlag, Heidelberg.

Bichara, M., & Fuchs, R. P. P. (1985) *J. Mol. Biol. 183*, 341–351.

Broyde, S., & Hingerty, B. E. (1983) *Biopolymers 22*, 2423–2441.

Broyde, S., & Hingerty, B. E. (1984) *Colloq. Biol. Sci., 1st 435*, 119–122.

Broyde, S., & Hingerty, B. E. (1987) *Nucleic Acids Res. 15*,

6539−6552.
Carothers, A. M., Urlaub, G., Mucha, J., Yuan, W., Chasin, L. A., & Grunberger, D. (1993) *Carcinogenesis 14*, 2181−2184.
Caruthers, M. H., Barone, A. D., Beaucage, S. L., Dodds, D. R., Fisher, E. F., McBride, L. J., Matteucci, M., Stabinsky, Z., & Tang, J.-Y. (1987) *Methods Enzymol. 154*, 287−313.
Cho, B. P., Beland, F. A., & Marques, M. M. (1994) *Biochemistry 33*, 1373−1384.
Clore, G. M., & Gronenborn, A. M. (1985) *FEBS Lett. 179*, 187−198.
Eckel, L. M. (1994) Structural Characterization of an *N*-2-Aminofluorene Modified Model *ras* Protooncogene DNA Oligomer by NMR Spectroscopy and Energy Minimization Calculations, Ph.D. Thesis, University of Rochester, Rochester, NY.
Eckel, L. M., & Krugh, T. R. (1994) *Nat. Struct. Biol. 1*, 89−94.
Evans, F. E., Miller, D. W., & Beland, F. A. (1980) *Carcinogenesis 1*, 955−959.
Evans, F. E., Miller, D. W., & Levine, R. A. (1986) *J. Biomol. Struct. Dyn. 3*, 935−948.
Fuchs, R., & Daune, M. (1972) *Biochemistry 11*, 2659−2666.
Fuchs, R. P., & Daune, M. P. (1974) *Biochemistry 13*, 4435−4440.
Fuchs, R. P. P., & Seeberg, E. (1984) *EMBO J. 3*, 757−760.
Garcia, A., Lambert, I. B., & Fuchs, R. P. P. (1993) *Proc. Natl. Acad. Sci. U.S.A. 90*, 5989−5993.
Grunberger, D., Nelson, J. H., Cantor, C. R., & Weinstein, I. B. (1970) *Proc. Natl. Acad. Sci. U.S.A. 66*, 488−494.
Gupta, R. C., & Dighe, N. R. (1984) *Carcinogenesis 5*, 343−349.
Hingerty, B. E., & Broyde, S. (1982) *Int. J. Quantum Chem. 9*, 125−136.
Hingerty, B. E., & Broyde, S. (1986) *J. Biomol. Struct. Dyn. 4*, 365−372.
Hore, P. J. (1983) *J. Magn. Reson. 55*, 283−300.
Huang, G., & Krugh, T. R. (1990) *Anal. Biochem. 190*, 21−25.
Johnson, D. L., Reid, T. M., Lee, M.-S., King, C. M., & Romano, L. J. (1987) *Carcinogenesis 8*, 619−623.
Kalnik, M. W., Norman, D. G., Zagorski, M. G., Swann, P. F., & Patel, D. J. (1989) *Biochemistry 28*, 294−303.
Kornberg, A., & Baker, T. A. (1992) *DNA Replication*, 2nd ed., W. H. Freeman, New York.
Kriek, E. (1992) *J. Cancer Res. Clin. Oncol. 118*, 481−489.
Kriek, E., & Spelt, C. E. (1979) *Cancer Lett. 7*, 147−154.
Krugh, T. R. (1973) *J. Am. Chem. Soc. 95*, 4761−4762.
Leng, M., Ptak, M., & Rio, P. (1980) *Biochem. Biophys. Res. Commun. 96*, 1095−1102.
Lipkowitz, K. E., Chevalier, T., Widdifield, M., & Beland, F. A. (1982) *Chem. Biol. Interact. 40*, 57−76.
Lutgerink, J. T., Retél, J., Westra, J. G., Welling, M. C., Loman, H., & Kreik, E. (1985) *Carcinogenesis 6*, 1501−1506.
Mah, M. C.-M., Maher, V., Thomas, H., Reid, T. M., King, C. M., & McCormick, J. J. (1989) *Carcinogenesis 10*, 2321−2328.
Michaels, M. L., Reid, T. M., King, C. M., & Romano, L. J. (1991) *Carcinogenesis 12*, 1641−1646.
Miller, J. A. (1970) *Cancer Res. 30*, 559−576.
Miller, J. A., & Miller, E. C. (1969) *Prog. Exp. Tumor Res. 11*, 273−301.
Morden, K. M., Chu, Y. G., Martin, F. H., & Tinoco, J. I. (1983) *Biochemistry 22*, 5557−5563.
Morgan, A. R. (1993) *Trends Biochem. Sci. 18*, 160−163.
Norman, D., Abuaf, P., Hingerty, B. E., Live, D., Grunberger, D., Broyde, S., & Patel, D. (1989) *Biochemistry 28*, 7462−7476.
O'Handley, S. F., Sanford, D. G., Xu, R., Lester, C. C., Hingerty, B. E., Broyde, S., & Krugh, T. R. (1993) *Biochemistry 32*, 2481−2497.
Poirier, M. C., True, B., & Laishes, B. A. (1982) *Cancer Res. 42*, 1317−1321.
Reid, T. M., Lee, M.-S., & King, C. M. (1990) *Biochemistry 29*, 6153−6161.
Sage, E., & Leng, M. (1980) *Proc. Natl. Acad. Sci. U.S.A. 77*, 4597−4601.
Sage, E., Spodheim-Maurizot, M., Rio, P., Leng, M., & Fuchs, R. P. P. (1979) *FEBS Lett. 108*, 66−68.
Sandström, J. (1982) *Dynamic NMR Spectroscopy*, Academic Press, New York.
Santella, R. M., Kriek, E., & Grunberger, D. (1980) *Carcinogenesis 1*, 897−902.
Selkirk, J. K. (1980) *Chemical Carcinogenesis: A Brief Overview of the Mechanism of Action of Polycyclic Hydrocarbons, Aromatic Amines, Nitrosamines, and Aflatoxins*, Raven Press, New York.
Shibutani, S., & Grollman, A. P. (1993) *J. Biol. Chem. 268*, 11703−11710.
Shibutani, S., Gentles, R. G., Iden, C. R., & Johnson, F. (1990) *J. Am. Chem. Soc. 112*, 5667−5668.
Shibutani, S., Gentles, R., Johnson, F., & Grollman, A. P. (1991) *Carcinogenesis 12*, 813−818.
Singer, B., & Grunberger, D. (1983) *Molecular Biology of Mutagens and Carcinogens*, Plenum, New York.
Sklenar, V., & Bax, A. (1987) *J. Magn. Reson. 74*, 469−479.
Sklenar, V., Brooks, B. R., Zon, G., & Bax, A. (1987) *FEBS Lett. 216*, 249−252.
Spodheim-Maurizot, M., Saint-Ruf, G., & Leng, M. (1979) *Nucleic Acids Res 6*, 1683−1694.
Tang, M. S., Lieberman, M. W., & King, C. M. (1982) *Nature 299*, 646.
van de Poll, M. L. M., Lafleur, M. V. M., van Gog, F., Vrieling, H., & Meerman, J. H. N. (1992) *Carcinogenesis 13*, 751−758.
van de Ven, F. J. M., & Hilbers, C. W. (1988) *Eur. J. Biochem. 178*, 1−38.
van Houte, L. P. A., Westra, J. G., Retél, J., van Grondelle, R., & Blok, J. (1987) *Carcinogenesis 9*, 1017−1027.
van Houte, L. P. A., Westra, J. G., Retél, J., & van Grondelle, R. (1988) *Carcinogenesis 9*, 1017−1027.
van Houte, L. P. A., van Grondelle, R., Retél, J., Westra, J. G., Zinger, D., Sutherland, J. C., Kim, S. K., & Geacintov, N. E. (1989) *Photochem. Photobiol. 49*, 387−394.
van Houte, L. P. A., Westra, J. G., Retél, J., & van Grondelle, R. (1991) *J. Biomol. Struct. Dyn. 9*, 45.
Vousden, K. H., Bos, J. L., Marshall, C. J., & Phillips, D. H. (1986) *Proc. Natl. Acad. Sci. U.S.A. 83*, 1222−1226.
Weinstein, B. (1981) *J. Supramol. Struct. Cell. Biochem. 17*, 107−128.
Weisburger, E. K., & Weisburger, J. H. (1958) *Adv. Cancer Res. 1*, 339−396.
Wemmer, D. E. (1992) *Biol. Magn. Reson.*, 195−264.
Wilson, R. H., DeEds, F., & Cox, A. J. (1941) *Cancer Res. 1*, 595−608.
Wiseman, R. W., Stowers, S. J., Miller, E. C., Anderson, M. W., & Miller, J. A. (1986) *Proc. Natl. Acad. Sci. U.S.A. 83*, 5825−5829.
Wüthrich, K. (1986) *NMR of Protein and Nucleic Acids*, John Wiley and Sons, New York.
Zhou, N., & Vogel, H. J. (1993) *Biochemistry 32*, 637−645.
Zhou, Y., & Romano, L. J. (1993) *Biochemistry 32*, 14043−14052.